12.2;13.3

Effect of electron beam energy on charging characteristics of polymer composites with the inclusion of carbon nanotubes

© E.A. Vorobyeva[1,2], A.P. Evseev[1,3], A.A. Tatarintsev[3], D.O. Peshnina[1], A.A. Shemukhin[1,3]

[1] Skobeltsyn Institute of Nuclear Physics, Moscow State University, Moscow, Russia
[2] National Research Center „Kurchatov Institute“, Moscow, Russia
[3] Faculty of Physics, Moscow State University, Moscow, Russia
E-mail: vorkate89@mail.ru

Received March 15, 2023
Revised April 28, 2023
Accepted April 29, 2023

The possibility of using polymer composite materials based on epoxy resins with the inclusion of carbon nanotubes as coatings with a low coefficient of secondary electron emission has been studied. Four types of samples were obtained: epoxy polymer, polymer composites with fillers (non-aligned and aligned carbon nanotubes, carbon soot). It is shown that the secondary electron emission yield depends on the structure of the introduced carbon filler, and polymer composites with aligned nanotubes exhibit antidynatron properties.

Keywords: multi-walled carbon nanotubes, nanocomposites, electron beam, secondary electron emission.

DOI: 10.61011/TPL.2023.06.56385.19556

Nanocomposites are a new type of dispersion materials with fine nanoscale material particles introduced into the bulk of a matrix. The matrix specifies mechanical properties of such materials, and their functional (optical, semiconductor, absorption) properties are governed by nanocomponents. Recent studies have addressed the issues of development of polymer nanocomposites with the inclusion of carbon nanotubes (CNTs) [1,2]. The interest in CNTs as a filler stems largely from their high thermal and electrical conductivity, fine mechanical properties, and chemical and thermal stability [3]. Such composites may be used as semiconductor materials [4,5], aerospace materials [6,7], sensors [8], sensor materials for self-diagnostics [9], and antibacterial coatings [10].

In the present study, we consider the application of polymer composites with the inclusion of multi-walled carbon nanotubes (MWCNTs) as coatings with a low coefficient of secondary electron emission. Secondary electron emission (SEE), which unwanted in certain applications, proceeds on the surface of materials exposed to an electron beam. For example, SEE in high-energy colliders, storage rings, and damping rings induces the formation of electron clouds, which interfere with their operation. CERN researchers have proposed to mitigate this problem by applying thin films of amorphous carbon with a low secondary electron yield [11]. Prototype coatings of this type are already being tested at the accelerator. At an energy of 1.8 keV, these carbon coatings provide a SEE coefficient of about 0.8, whereas the coefficient for stainless steel at the same energy is 1.4. Such antidynatron coatings may also be used in electron spectrometers, collectors of secondary electrons downstream of microchannel plates [12], and other devices monitoring ion or electron currents. Low-SEE coatings are needed to construct equipment for Earth remote probing in space flights, where a resonance radio-frequency discharge is initiated in vacuum and sustained by secondary electron emission from the walls of high-frequency instruments. Secondary electrons emitted from surfaces induce an electron avalanche. Coatings with a SEE coefficient remaining below unity within the entire range of energies of primary electrons are needed to mitigate this effect [13].

The following samples were synthesized and examined in the present study in order to determine SEE coefficients: polymer composite materials based on epoxy resins with 0.9 and 2.7% (by mass) of carbon nanotubes; polymer composite materials based on epoxy resins with 0.9 and 2.7% (by mass) of carbon soot; and a polymer composite material based on epoxy resins with aligned MWCNTs (two batches).

A polymer binder (epoxy resin L) and hardener 285 (LBA Epoxy resin L 285) were used to fabricate the samples. „Taunit“ carbon nanotubes or soot were admixed into the polymer matrix. Ultrasonic treatment was performed to achieve a uniform distribution of CNTs within the polymer matrix. Thin discs were formed from the obtained composite and polymerized for 24 h at room temperature. The mass percentage of CNTs (soot) in different samples was 0.9 or 2.7%. Samples with aligned CNTs were prepared by pyrolytic gas-phase deposition. A sample was initially an array of MWCNTs aligned perpendicularly to a substrate. Polymer was deposited onto the sample surface in small droplets. Following polymerization within 24 h, the composite was exfoliated from the silicon substrate, and the upper polymer layer containing no nanotubes was polished away with a diamond abrasive brick to expose

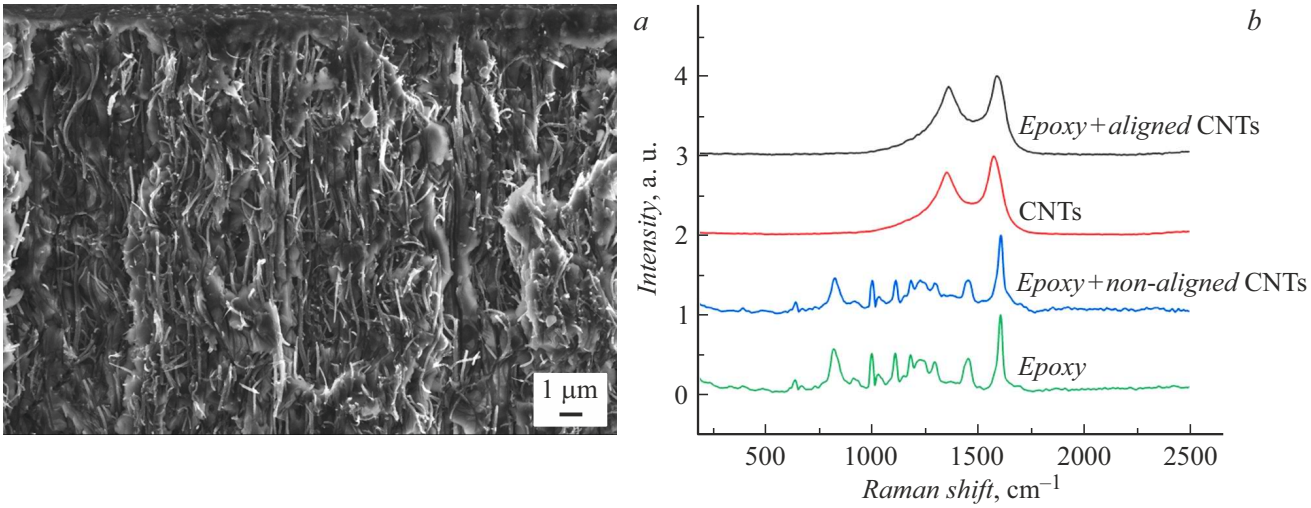

Figure 1. *a* — SEM image of the polymer composite based on epoxy resins with the inclusion of aligned carbon nanotubes. *b* — Raman spectra of the polymer, CNTs, and the polymer composite with aligned and non-aligned CNTs.

the composite with CNTs. Since the mean diameter of aligned CNTs was 40 nm and the distance between their centers was 200 nm, the volume fraction of CNTs was approximately 3%.

The obtained samples were examined with a scanning election microscope (SEM) and studied using Raman spectroscopy, which turns out to be efficient in detection of CNTs in concentrations upward of 0.5% in nanocomposites [14]. It has already been demonstrated that an increase in concentration of nanocomponents in a composite leads to enhancement of the functional properties of a sample [15].

The SEM image in Fig. 1, *a* demonstrates that nanotubes rise to the surface of the composite. Figure 1, *b* presents the Raman spectra of multi-walled carbon nanotubes, the polymer. and the polymer composite with CNTs. The Raman spectrum of the epoxy resin features a large number of weakly pronounced peaks, which is typical of polymers [16]. The spectrum of pure CNTs is characterized by the presence of D peaks (around 1350 cm^{-1}), which emerge due to the presence of defects and disordering in graphite-like materials, and G peaks (around 1550–1600 cm^{-1}). The peak at a frequency of 1582 cm^{-1} in graphite corresponds to tangential vibrations of carbon atoms. The intensity of the G peak is regarded as an indicator of graphitization. These CNT peaks overlap partially with the epoxy resin peaks. The spectrum of the composite with non-aligned CNTs features a multitude of weakly pronounced peaks, which are similar in shape and position to those present in the spectrum of the epoxy resin. The D and G peaks for the composite with aligned CNTs are similar to those observed for pure CNTs, but their positions are shifted. Thus, it may be concluded that the ends of carbon nanotubes are present on the composite surface. The shift of carbon vibrations in the composite with CNTs toward higher frequencies (relative to the spectrum of pure CNTs) is indicative of compressive strain of CNTs [17]. For example, the authors of [18] have estimated the Young's modulus of MWCNTs by measuring the shift of the G' peak of MWCNTs in an epoxy resin.

Charging of the synthesized samples under electron irradiation was examined using an electron-probe measurement complex based on an electron microscope (the procedure was detailed in [19,20]) at a primary beam current of 100 pA to an irradiation region 100 × 100 μm in size, which yields charging current density $j_0 = 10^{-7}$ A/cm^2. The experiment was focused on measuring emission current I_σ with a hemispherical electron collector. A nanoammeter was also used to monitor current I_{L+D} from the sample holder, which is the sum of the displacement current (accumulated charge) and the leakage current. Since the sum of current I_σ from the hemispherical electron collector and current I_{L+D} from the sample holder is equal to incident beam current $I_0 = I_\sigma + I_{L+D}$, the dynamics of current from the substrate is correlated with the emission current and is a monitoring variable. Experiments were performed at primary electron beam energies varying from 0.2 to 15 keV. Time dependences of secondary electron emission current I_σ and the sum displacement current were measured within the range of incident electron beam energies from 0.2 to 15 keV to examine the process of charging. The pure polymer material without inclusions charges rapidly at all the examined irradiation energies (Fig. 2, *a*); current I_{L+D} reaches an equilibrium magnitude within $\sim 10-15$ s even at relatively low current densities. The SEE current grows fast to $I_\sigma = I_0 - I_{L+D} \approx 100$ pA, with is a classical case for charging of dielectrics with the resulting SEE coefficient $\sigma \approx 1$.

At an electron energy of 15 keV, the polymer composite with non-aligned CNTs starts to deviate in charging char-

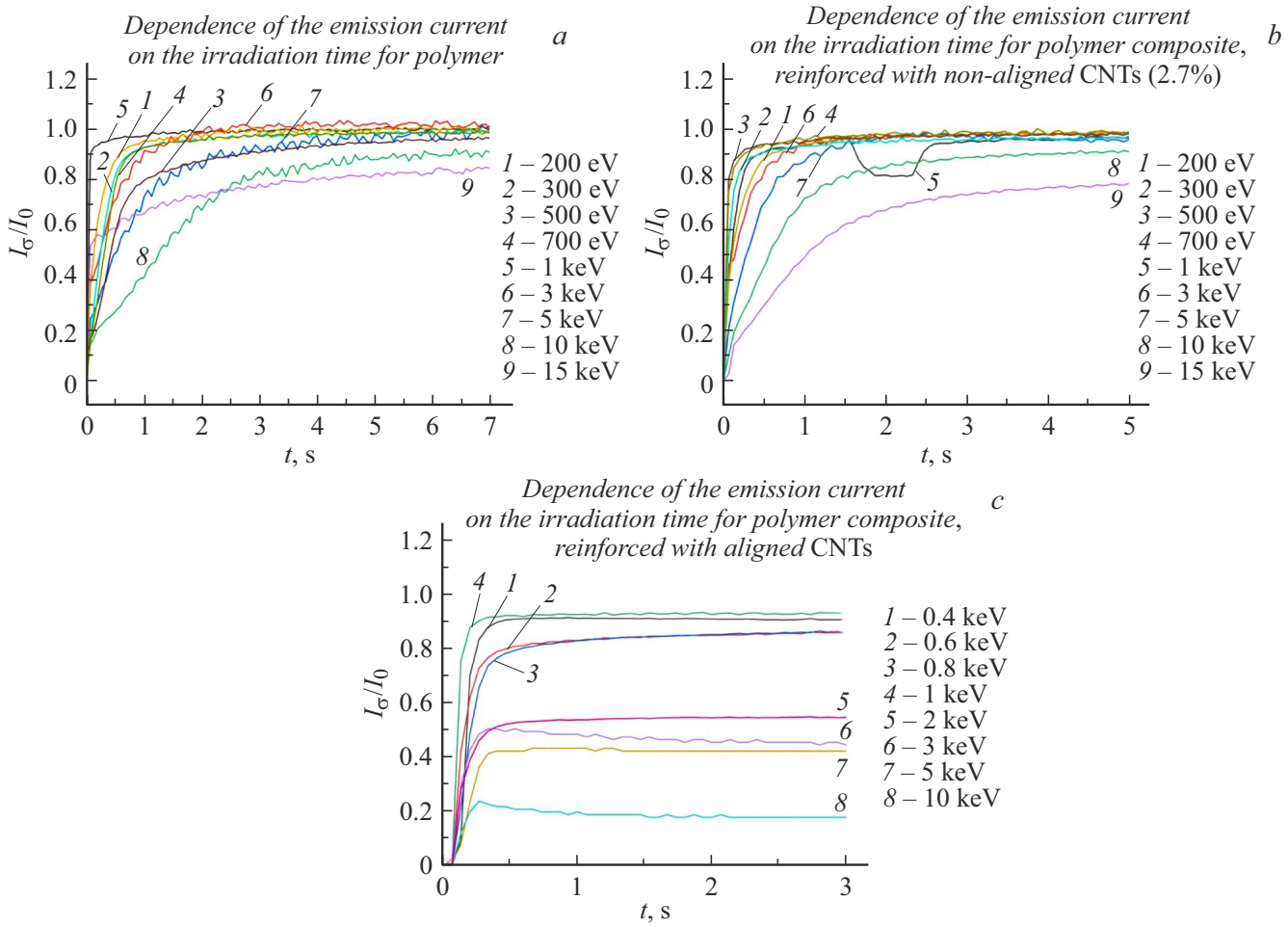

Figure 2. Dependence of emission current I_σ/I_0 on the irradiation time for a range of incident electron energies of 0.2–15 keV for the polymer (a) and polymer composites with non-aligned (b) and aligned (c) CNTs.

acteristics from the pure polymer: current $I_{L+D} = 17$ pA for the polymer with CNTs and 11 pA for the pure polymer (Fig. 2, b). The secondary electron emission current is 70 pA for the composite with a mass percentage of CNTs of 2.7%, 82 pA for the composite with 0.9% of CNTs, and 85 pA for the pure resin. It should be noted that antidynatron properties get enhanced by 10% when the mass percentage of non-aligned carbon nanotubes in the polymer matrix increases by a factor of 3. A weakly pronounced antidynatron effect was also observed at high electron beam energies in experiments with polymer composites containing 0.9 and 2.7% of soot (by mass).

Let us consider the process of charging of the polymer composite with aligned CNTs (Fig. 2, c). Almost no charging is observed in this case at high energies. The secondary electron spectrum behaves like the spectrum of metallic samples: the spectrum shift is zero. Current I_{L+D} from the substrate at a primary electron beam energy of 15 keV is close to 85% of the incident beam current. The remaining electrons are reflected and secondary ones. The composite charges at low primary electron beam energies (up to 1 keV). However, the current from the substrate for primary electron beam energies of 3 and 5 keV is just around 60% of the incident current. Such a dependence is typical of the SEE spectrum of dielectrics. Similar experiments were performed for the second batch of polymer composites with the inclusion of aligned CNTs. Figure 3 shows clearly that polymer nanocomposites with aligned CNTs are the most efficient in suppressing the secondary electron emission: the SEE coefficient at high energies is 0.1–0.3.

It was demonstrated that a polymer material exhibits antidynatron properties after the introduction of aligned CNTs into it: no charging is observed, and the secondary electron spectrum behaves like the spectrum of metallic samples (the spectrum shift is zero). Thus, polymers with the inclusion of aligned CNTs may be used to produce coatings with a low SEE coefficient. The obtained coefficient is lower than the ones reported in literature for amorphous carbon coatings that are used to prevent the formation of electron clouds in particle accelerators.

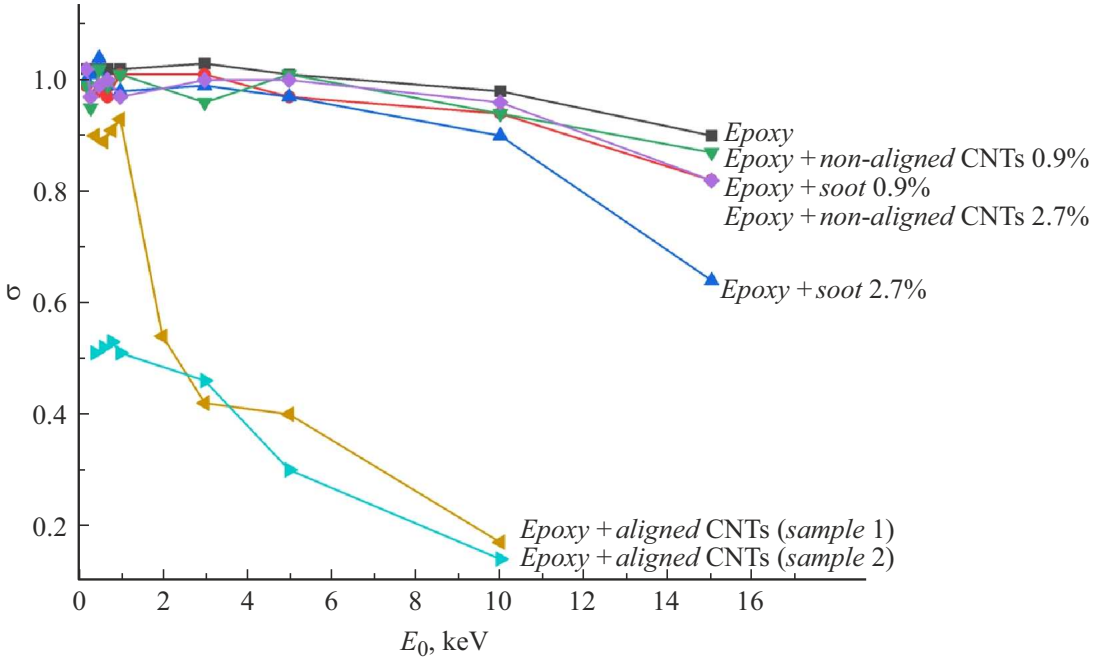

Figure 3. Dependence of the secondary electron emission coefficient on the energy of an incident electron beam for the polymer, the polymer composite with the inclusion of 0.9% of non-aligned CNTs, the polymer composite with the inclusion of 0.9% of soot, the polymer composite with the inclusion of 2.7% of non-aligned CNTs, the polymer composite with the inclusion of 2.7% of soot, and the polymer composite with the inclusion of aligned CNTs (sample batches 1 and 2).

Funding

This study was supported financially by the Russian Science Foundation, project No. 21-79-00190.

Conflict of interest

The authors declare that they have no conflict of interest.

References

[1] A. Hosseinzadeh, S. Bidmeshkipour, Y. Abdi, E. Arzi, S. Mohajerzadeh, Appl. Surf. Sci., **448**, 71 (2018). DOI: 10.1016/j.apsusc.2018.04.099
[2] L. Camilli, M. Passacantando, Chemosensors, **6**, 62 (2018). DOI: 10.3390/chemosensors6040062
[3] S. Ren, P. Rong, Q. Yu, Ceram. Int., **44**, 11940 (2018). DOI: 10.1016/j.ceramint.2018.04.089
[4] F. Rigoni, C. Pintossi, G. Drera, S. Pagliara, G. Lanti, P. Castrucci, M. de Crescenzi, L. Sangaletti, Sci. Rep., **7**, 44413 (2017). DOI: 10.1038/srep44413
[5] A. di Bartolomeo, Phys. Rep., **606**, 1 (2016). DOI: 10.1016/J.PHYSREP.2015.10.003
[6] L. Vertuccio, F. De Santis, R. Pantani, K. Lafdi, L. Guadagno, Composites B, **162**, 600 (2019). DOI: 10.1016/J.COMPOSITESB.2019.01.045
[7] L. Gorbatikh, B.L. Wardle, S.V. Lomov, MRS Bull., **41**, 672 (2016). DOI: 10.1557/mrs.2016.170
[8] D. Wentzel, S. Miller, I. Sevostianov, Int. J. Eng. Sci., **120**, 63 (2017). DOI: 10.1016/j.ijengsci.2017.06.013
[9] F. Wang, S. Liu, L. Shu, X.M. Tao, Carbon, **121**, 353 (2017). DOI: 10.1016/j.carbon.2017.06.006
[10] M. Azizi-Lalabadi, H. Hashemi, J. Feng, S.M. Jafari, Adv. Colloid Interface Sci., **284**, 102250 (2020). DOI: 10.1016/J.CIS.2020.102250
[11] C.Y. Vallgren, G. Arduini, J. Bauche, S. Calatroni, P. Chiggiato, K. Cornelis, P. Costa Pinto, B. Henrist, E. Métral, H. Neupert, G. Rumolo, E. Shaposhnikova, M. Taborelli, Phys. Rev. ST Accel. Beams, **14**, 071001 (2011). DOI: 10.1103/PhysRevSTAB.14.071001
[12] A.T. Dideykin, E.D. Eidelman, A.Ya. Vul', Solid State Commun., **126**, 495 (2003). DOI: 10.1016/S0038-1098(03)00253-9
[13] I. Montero, L. Olano, L. Aguilera, M.E. Dávila, U. Wochner, D. Raboso, P. Martıin-Iglesias, J. Electron Spectrosc. Relat. Phenom., **241**, 146822 (2020). DOI: 10.1016/J.ELSPEC.2019.02.001
[14] Y. Piao, V.N. Tondare, C.S. Davis, J.M. Gorham, E.J. Petersen, J.W. Gilman, K. Scott, A.E. Vladár, A.R. Hight Walker, Compos. Sci. Technol., **208**, 108753 (2021). DOI: 10.1016/j.compscitech.2021.108753
[15] J.-F. Brun, C. Binet, J.-F. Tahon, A. Addad, P. Tranchard, S. Barrau, Synth. Met., **269**, 116525 (2020). DOI: 10.1016/j.synthmet.2020.116525
[16] D. Griffin, S. Wood, I. Hamerton, Composites B, **200**, 108210 (2020). DOI: 10.1016/J.COMPOSITESB.2020.108210
[17] V.G. Hadjiev, G.L. Warren, L. Sun, D.C. Davis, D.C. Lagoudas, H.-J. Sue, Carbon, **48**, 1750 (2010). DOI: 10.1016/J.CARBON.2010.01.018

[18] A. Aoki, T. Ogasawara, T. Aoki, Y. Ishida, Y. Shimamura, Y. Inoue, Composites A, **167**, 107448 (2023). DOI: 10.1016/J.COMPOSITESA.2023.107448
[19] E.I. Rau, A.A. Tatarintsev, Phys. Solid State, **63** (4), 628 (2021). DOI: 10.1134/S1063783421040181.
[20] A.A. Tatarintsev, K.E. Markovets, E.I. Rau, J. Phys. D: Appl. Phys., **52**, 115104 (2019). DOI: 10.1088/1361-6463/aafbfc.

Translated by D.Safin